AEROSOL SCIENCE AND TECHNOLOGY
2017, VOL. 0, NO. 0, 1–9
http://dx.doi.org/10.1080/02786826.2017.1316829

Taylor & Francis
Taylor & Francis Group

A contribution to the amaranthine quarrel between true and average electrical mobility in the free molecular regime

Carlos Larriba-Andaluz, Minal Nahin, and Vaibhav Shrivastav

Department of Mechanical Engineering, IUPUI, Indianapolis, Indiana, USA

ABSTRACT

Landau and Lipschitz's approach—termed here H&B due to the use of Happel and Brenner's slow rotation approximation—for calculating the average electrical mobility over all orientations of an ion in the free molecular regime is shown in this manuscript to be an invalid assumption for non-globular ions when a fixed electrical field is present. The reason behind the invalidity seems to be the confusion between average "settling" velocity (the calculation intended by H&B) and the average mobility(drag) in the direction of the field. When a missing orientation is taken into account by rotating the drag tensor, the average mobility obtained through Landau's approach coincides with well-known orientationally averaged Kinetic Theory Methods such as those of Mason and McDaniel (M&M). H&B's averaging approach, however, can be related to the true mobility displacement of the ion or, in other words, the displacement occurring in the direction of the velocity. This true mobility displacement only agrees with the average mobility displacement if ion velocity and electrical field have always the same direction, which only happens under special cases. Analytical and numerical calculations of collision cross-sections of linear and planar structures using a momentum transfer kinetic theory approach are chosen here as a means to prove that a single rotation of the drag tensor is sufficient to show agreement between both methods. A projected area approach is also used to prove the inadequacy of the H&B method.

ARTICLE HISTORY
Received 6 November 2016
Accepted 29 March 2017

EDITOR
Yannis Drossinos

I. Introduction

From a semi-classical point of view, it is becoming more self-evident that there is a need to understand the microscopical behavior of systems in order to correctly define transport and thermofluid properties. It is far more evident that as science and technology progresses, the need to accurately define these properties could signify the difference between correct and incorrect modeling. In the free molecular regime, most transport properties are defined using a "directional" cross-section defined by the interaction of the species of interest with the surrounding medium. The ensemble average of all possible orientations, speeds, and fundamental force interactions define the collision integral or the collision cross-section (CCS), which can then be used to define the mobility diameter. Among many of such CCS-defined transport properties, electrical mobility is extensively used in the physical characterization of ions, clusters, and nanometer-sized aerosol particles (de la Mora et al. 1998; Bohrer et al. 2008). Under standard temperatures and pressures, Knudsen numbers of nanometer-scale particles that move at slow velocities fall within the momentum transfer free molecular regime, in which ion mobility, i.e., the average drift velocity acquired per unit electrical field experimented by a charged ion, can be expressed using the Mason–Schamp equation (Mason and McDaniel 1988):

$$Z_p = \sqrt{\frac{\pi m_{red}}{8kT}}\frac{3ze}{4\rho_{gas}\Omega}, \qquad [1]$$

where m_{red} is the reduced mass, k is Boltzmann's constant, T is the temperature, z is the net number of integer (positive or negative) charges on the particle, e is the unit charge, ρ_{gas} is the density, and Ω is the particle's averaged collision cross-section. The collision cross-section Ω is a gas momentum-transfer-based collision integral that is orientationally averaged, i.e., calculates all gas molecule impingements onto an ion that is randomly oriented. Equation (1) is the basics of gas dynamics and has been extensively used analytically and numerically to infer collision cross-sections and mobilities (Shvartsburg and Jarrold 1996; Ruotolo et al. 2008; Pease et al. 2009; Tsai et al. 2009; Hogan and de la Mora 2011; Jiang et al. 2011; Larriba et al. 2011; Larriba and de la Mora 2012; Larriba et al. 2014).

Arguably, the most accepted simplifications for acquiring an average Ω for an ion or aerosol nanoparticle are (1) the consideration that all directions are equally probable and (2) that non-inertial effects can be ignored. The

first of such simplifications has had the most controversy in the last few years due to the application of two different approaches. The first approach follows the work of Mason and McDaniel (M&M; Li and Wang 2003a,b) based on Chapman-Enskog's theory, which defines an orientationally averaged collision integral and agrees with Equation (1). The second approach, which we will refer to as the Happel and Brenner method (H&B; Epstein 1924; Happel and Brenner 1981; Landau and Lifshitz 1987), is a momentum transfer approach that calculates a drag tensor for the particle of interest. This drag tensor is positive definite, when dynamic effects of rotation are neglected, and therefore can be diagonalized and, if inverted, an average value of the mobility, and thus of the collision cross-section, is said to be found by averaging the sum of the trace of the inverse tensor (see Landau and Lifschitz, equation 59-6). The controversy relies in the fact that these two methods (M&M and H&B) do not yield the same results even though both methods have been amply supported (Dahneke 1973a,b; Chan and Dahneke 1981; Landau and Lifshitz 1987; Garciaybarra and Rosner 1989; Bird 1994; Mackowski 1994, 2006; Tammet 1995; Mesleh et al. 1997; Shvartsburg et al. 1997; de la Mora 2002; Garcia-Ybarra et al. 2006; Larriba and Hogan 2013a,b; Li et al. 2014a,b).

In this work, it is shown that the drag tensor calculated in H&B, when used to calculate the average mobility in the direction of the field, does not consider all possible orientations of the ion (H&B section 5–2.12) and that a small geometrical consideration leads to both approaches being equivalent. Averaging the inverted tensor using the H&B approach (H&B section 5–8) does however have a physical meaning that is equivalent to calculating the average settling velocity—probably the one intended by H&B and perhaps later misinterpreted. The total displacement in the direction of the velocity is termed here true displacement and its value differs from the average mobility displacement in the direction of the field. Theory is corroborated first analytically using a cylinder/disk and later on through numerical calculations using *IMoS* (Zhang et al. 2012; Larriba-Andaluz and Hogan 2013; Ouyang et al. 2013; Larriba-Andaluz and Hogan 2014; Larriba-Andaluz et al. 2015; Oberreit et al. 2015), an all-atom momentum transfer model that can mimic both approaches, H&B and M&M (see the online supplementary information [SI] for results in calculations). Although not pursued in this work, special attention should be taken when using the mean diffusivity (Basser et al. 1994; Alexander et al. 2007; Basser and Pierpaoli 2011), which can lead to averaging errors for planar and linear ions due to the similarities between diffusion and electrical mobility (Einstein's relation). Given that the charged particles studied herein this manuscript are large polyatomic entities (up to 5000 atoms), we will refer to them as ions, particles, or nanoparticles indistinctively with the only precaution that these ions must fall within the free molecular regime.

2. Theory

2.1. Average non-dynamic mobility of charged polyatomic nanoparticles when all orientations are equally probable

Let a random amorphous polyatomic charged structure with mass m and charge q be pulled by a constant electric field $\boldsymbol{E}$ in a gas medium. The resulting equation of motion (for slow velocities) is given by

$$m\ddot{\vec{x}} = q\vec{E} - \overline{\overline{K}}\dot{\vec{x}} \ , \qquad [2]$$

where the translational inertia of the ion is given by the balance of the electrical force, $q\vec{E}$, and the collision-induced drag force, $\overline{\overline{K}}\dot{\vec{x}}$. One can argue that the equilibration between the forces will happen fast enough that the LHS will almost immediately become negligible under small changes in velocity. In order for such equilibration to happen, one can also hypothesize that the speed of rotation of the nanoparticle must not significantly affect singular collisions between gas molecule and ion. In order to simplify the picture, let us assume the following hypotheses:

(i) The particle reaches terminal velocity instantly. This terminal velocity and its direction are determined by the equilibrium of forces in Equation (2). After terminal velocity is reached, any inertial acceleration, rotational or translational, is assumed to be negligible.
(ii) All orientations of the ion are equally probable.
(iii) For (ii) to be true, the nanoparticle is continuously reorienting itself after a random number of gas collisions as it drifts through space. This reorientation happens enough to allow pure statistical randomness.
(iv) The nanoparticle speed of rotation can have any value as long as it is slow enough that the angular velocity of the nanoparticle contributes negligibly to the momentum transfer upon collision of a gas molecule with the ion. If the ion speed of rotation is high, individual collisions with gas molecules would be affected by the speed of rotation and the analysis assumed herein would need to be modified.
(v) The averaged drift velocity ($<v_i>$) under assumptions (i) through (iv) must be in the direction of the electrical field (E_i).

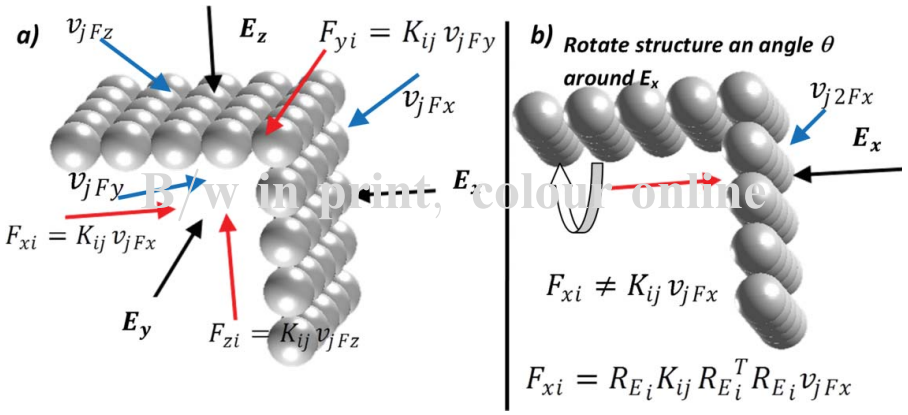

Figure 1. (a) Given a molecular structure with a fixed orientation, one can infer the tensor K_{ij} from three perpendicular directions (*Ex, Ey, Ez*). Black arrows correspond to the direction of the field, red arrows correspond to the drag force response, and blue arrows correspond to the drift velocity resulting from the equilibrium. Only one drift velocity v_j can be produced from each drag-Field pair for a given K_{ij}, i.e., $F_{xi} = K_{ij} v_{jF_x}$. (b) A rotation of the ion around E_x should still produce the same reaction F_x but a different drift velocity v_{j2}. The tensor K_{ij} does not contain this orientation of the ion so that $K_{ij} v_{j2F_x}$ will not produce F_{xi}. Instead a rotation of the tensor must also be made to produce this new orientation $F_{xi} = R_{E_i} K_{ij} R_{E_i}^T R_{E_i} v_{jF_x}$.

Under these hypotheses, both forces, electrical and drag must be equal in direction and magnitude at all times during the flight (in Einstein's notation):

$$qE_i = F_{Di} = K_{ij} v_j. \qquad [3]$$

Given that, when neglecting angular velocity (hypothesis iv), the drag tensor K_{ij} is symmetric, the tensor can be diagonalized and an average value calculated by assuming all orientations are equally probable. Since the tensor can be diagonalized, the average value is the sum of the trace divided by three.

Averaging leads to two options:

$$q \langle E_i \rangle = qE = \langle K_{ij} v_j \rangle \cong \langle K_{ij} \rangle \langle v_j \rangle, \qquad [4]$$

non-spherical ion, are given by

$$\overline{K_{ij}}^{-1} = \frac{Z_1}{q} = \frac{3}{K_{11} + K_{22} + K_{33}}, \qquad [4']$$

$$\overline{K_{ij}^{-1}} = \frac{Z_2}{q} = \frac{1}{3}\left(\frac{1}{K_{11}} + \frac{1}{K_{22}} + \frac{1}{K_{33}}\right); \qquad [5']$$

where K_{ii} are the principal directions of the tensor.

The purpose of this work is to understand the qualitative difference between both calculated mobilities Z_1 and Z_2. While a derivation will not be shown here, the calculation of the mobility using an orientationally averaged calculation, e.g., first collision integral, such as that of Mason and McDaniel, M&M, using Equation (1) agrees with averaging K_{ij} first (Equation (4)) and then inverting

$$R_{E_i} = \begin{bmatrix} \cos\theta + a^2(1-\cos\theta) & ab(1-\cos\theta) - c\sin\theta & ac(1-\cos\theta) + b\sin\theta \\ ab(1-\cos\theta) + c\sin\theta & \cos\theta + b^2(1-\cos\theta) & bc(1-\cos\theta) - a\sin\theta \\ ac(1-\cos\theta) - b\sin\theta & bc(1-\cos\theta) + a\sin\theta & \cos\theta + c^2(1-\cos\theta) \end{bmatrix}. \qquad [7]$$

$$q\left\langle \frac{E_i}{K_{ij}} \right\rangle = qE \langle K_{ij}^{-1} \rangle = \langle v_j \rangle; \qquad [5]$$

it (see analytical example). The average mobility using Equation (5) on the other hand agrees with the work of Landau and Lifschitz and that of Happel and Brenner, H&B. There has to be an underlying reason or a misconception to why these two ways of averaging lead to different mobility results.

The first possibility is to average the tensor K_{ij} directly by "assuming" that it is independent of the velocity and then inverting it. The second approach is to first invert the tensor and then take the average of the inverted tensor K_{ij}^{-1}. The two results, which differ for any

Given that Equation (3) is correct under given assumptions, how is it possible that averaging the tensor does not provide a mathematically correct description

$$D_{ij} = \begin{bmatrix} \frac{K_{11}}{2}A_a + \frac{K_{22}}{2}C_{abc} + \frac{K_{33}}{2}C_{acb} & Symm & Symm \\ \frac{ab}{2}(K_{11}B_a + K_{22}B_b + K_{33}B_c) & \frac{K_{22}}{2}A_b + \frac{K_{11}}{2}C_{abc} + \frac{K_{33}}{2}C_{bca} & Symm \\ \frac{ac}{2}(K_{11}B_a + K_{22}B_b + K_{33}B_c) & \frac{bc}{2}(K_{11}B_a + K_{22}B_b + K_{33}B_c) & \frac{K_{33}}{2}A_c + \frac{K_{11}}{2}C_{acb} + \frac{K_{22}}{2}C_{bca} \end{bmatrix},$$

regardless of whether the regular or inverse tensors are used? The answer, as will be shown, is that not all orientations are considered in Equation (3) and therefore averaging Equation (3) is not necessarily "equivalent to the assumption that all orientations are equally probable" and hypothesis (ii) will not be satisfied.

To mathematically calculate the drag tensor for a polyatomic ion with a fixed orientation, a possible option is to use three perpendicular directions to calculate the corresponding drag tensor K_{ij} (see analytical example of disk/cylinder). The electric field can be defined in Equation (3) as a function of two Euler angles (ϕ, χ) as $E_i = E(\sin\phi\ \cos\chi, \sin\phi\ \sin\chi, \cos\phi)$, so that for a fixed K_{ij} (with principal directions K_{11}, K_{22}, K_{33}):

$$qE(\sin\phi\ \cos\chi, \sin\phi\ \sin\chi, \cos\phi) = (K_{11}v_1, K_{22}v_2, K_{33}v_3), \quad [3']$$

where $v_j = (v_1, v_2, v_3)$. The velocity satisfying (3') is

$$v_j = \left(\frac{qE}{K_{11}}\sin\phi\ \cos\chi, \frac{qE}{K_{22}}\sin\phi\ \sin\chi, \frac{qE}{K_{33}}\cos\phi\right),$$

where the values qE/K_{ii} can be termed orientation weights. This process only uses *two* of the three Euler angles for a fixed tensor K_{ij}, which is key to the argument developed here. If one were to integrate Equation (3′) over the third angle, an angle of revolution along the E_i axis (termed θ), the equation would be invariant to the integration:

$$\int_0^{2\pi} qE_i d\theta = qE_i = \int_0^{2\pi} K_{ij}v_j d\theta = K_{ij}v_j. \quad [3'']$$

Except for particular cases, this cannot be the correct equation to average assuming all orientations are equally

$$D_{ij}' = \begin{bmatrix} K_{11}a^2 + K_{22}b^2 + K_{33}c^2 & 0 & 0 \\ 0 & K_{11}a^2 + K_{22}b^2 + K_{33}c^2 & 0 \\ 0 & 0 & K_{11}a^2 + K_{22}b^2 + K_{33}c^2 \end{bmatrix}. \quad [9]$$

probable as it is invariant under the integration of one of the angles. Imagine, for example, a simple finite θ rotation of the ion along the E_i axis. Physically, a new drift velocity is produced, v_{j2}, for the same E_i, which is not satisfied by Equation (3). Figure 1 provides detailed insight of the missing rotation for an L-shaped ion (used here to easily represent the rotation). Initially, Figure 1a shows an ion drag tensor that can be produced by randomly selecting three perpendicular directions of E_i. A new orientation that was not accounted for in Equation (3) is now provided in Figure 1b.

Therefore, to account for all possible orientations, one must include a rotation of the ion along the E_i axis. In such a case, Equation (3) can be rewritten as

$$qE_i = F_{Di} = \left(R_{E_i}K_{ij}R_{E_i}^T\right)\left(R_{E_i}v_j\right), \quad [6]$$

where R_{Ei} is the rotation matrix of an angle θ along a unit vector $\hat{u} = (a, b, c) = (\sin\phi\ cos\chi, sin\phi\ sin\chi, cos\phi)$ in the direction of E_i (or v_i):

The first term in brackets in the right-hand side of Equation (6) represents the rotation of the tensor K_{ij} while the second term in brackets represents the rotation of the velocity vector v_j. Equation (6) remains valid and equivalent to Equation (3) regardless of how much the ion is rotated along the E_i axis. Only one position of this particular θ-rotation would be

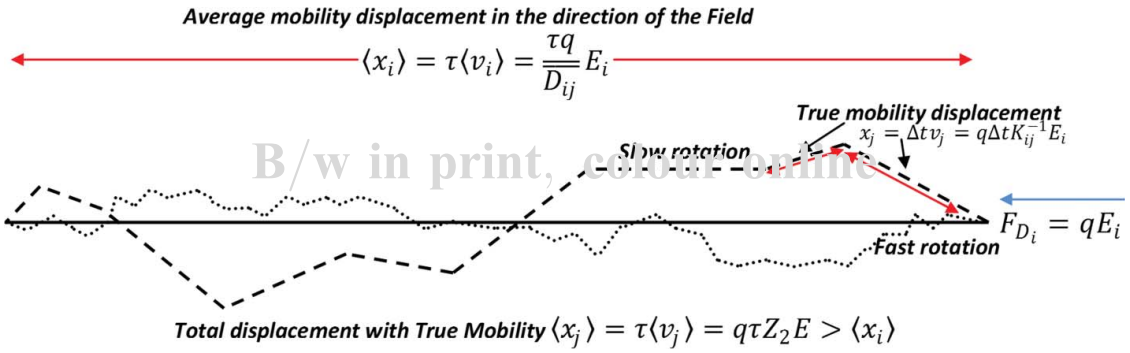

Figure 2. Shows the comparison between true and average displacements for two equivalent structures rotating fast (dotted line) and slow (dashed line). True mobility displacement is not in the direction of the Field but, when all directions are equally probable, the average displacement in the direction of the Field is given by $<x_i>$. On the other hand, true displacement x_j occurs in the direction of the velocity and is given by the true mobility Z_2. It must always be true that $<x_j> \geq <x_i>$. Δt is the time taken for a single rotation while τ is the total time to cover a given distance.

taken into account when only the tensor K_{ij} in Equation (3) is averaged. Since every θ-rotation is independent of each other, Equation (6) and not (3) should be employed and the resulting tensor, not K_{ij}, should be used when averaging.

To average such tensor, one can make use of Equation (6) to get the average θ-rotated tensor for a fixed E_i:

$$qE_i = F_{Di} = \overline{R_{E_i} K_{ij} R_{E_i}^T}\ \overline{R_{E_i} v_j} = \overline{R_{E_i} K_{ij} R_{E_i}^T} v_i = D_{ij} v_i. \quad [8]$$

Equation (8) needs further explanation to prove that the product of the averages is indeed the average of the products. The result can be proven by brute force. However, since the product of the averages, $D_{ij}v_i$, yields qE_i, as shown at the end of the derivation, the covariance must indeed be zero.

At a first glance, it is particularly interesting to note that the average of $R_{Ei}v_j$ is in this case always in the direction of the field (v_i) regardless of the value of v_j (average rotation along the E_i direction). The average value D_{ij} for that particular position of E_i (assuming K_{ij} is given as a diagonal matrix with three principal axes) is given by the following matrix:

where

$$A_i = (1 - 2i^2 + 3i^4)\ B_i = (3i^2 - 1)$$
$$C_{ijk} = 3i^2 j^2 + k^2$$

Since the tensor is symmetric and the product of $D_{ij}v_i$ must still be in the direction of v_i, diagonalizing the above matrix gives

Finally, averaging over all positions of vector $\hat{u}$:

$$\hat{u} = (\sin\phi\ \cos\chi, \sin\phi\ \sin\chi, \cos\phi) \quad [10]$$

gives

$$D_{ij}'' = \begin{bmatrix} \frac{K_{11}+K_{22}+K_{33}}{3} & 0 & 0 \\ 0 & \frac{K_{11}+K_{22}+K_{33}}{3} & 0 \\ 0 & 0 & \frac{K_{11}+K_{22}+K_{33}}{3} \end{bmatrix}. \quad [11]$$

Note that $\boldsymbol{u}$ is described as expected by only two angles (χ,ϕ) of the total three needed to describe the orientation of an object. It is true that in the derivation of H&B, a third Euler angle, with the same orientation as θ, is used to average the settling velocity. However, as shown in Equation (3″), Equation (3) is invariant under such rotation making the average of the angle meaningless. The average value of D_{ij}'' is

$$\overline{D_{ij}''} = \frac{K_{11}+K_{22}+K_{33}}{3}, \quad [12]$$

which coincides with q/Z_1 in Equation (4). The most significant property of D_{ij}'' is that the average of its inverse is $1/\langle D_{ij}'' \rangle$. It is therefore indifferent whether Equation (6) or

$$q\left(R_{E_i} K_{ij}^{-1} R_{E_i}^T\right)(E_i) = R_{E_i} v_j \quad [6']$$

is used. For a fixed field and when all orientations are taken into account, the Mobility is given by tensor M_{ij}

(to differentiate from Z) as

$$\overline{M_{ij}} = \frac{1}{\overline{D''_{ij}}} = \frac{3}{K_{11} + K_{22} + K_{33}}. \quad [13]$$

A general conclusion is therefore that when all orientations are considered and when the rotations that produce such orientations do not affect the gas molecule collisions, there is one and only one solution to calculating the average value of the mobility in the direction of the field and that is the one given by Equation (13). This result also agrees with that of M&M.

2.2. True vs. average mobility

So far, we have seen that the average mobility should be obtained by averaging the tensor D_{ij} and not the tensor K_{ij} (despite the coincidence). This average mobility is what is calculated in an ion mobility spectrometer (IMS). What remains to do now is to understand the reasoning behind why Equation (4) yields the same value as Equation (13) despite its averaging being in principle mathematically incorrect while Equation (5) yields a different value. To do so, let us first imagine an ion that travels a given distance with a fixed orientation. After such distance is covered, it instantly rotates and travels a new distance in a new fixed orientation. This is repeated until all orientations of the ion are covered. See Figure 2 for a sketch of the process.

Since Equation (6) must remain valid, then the true drift velocity of a particle along a path before rotating will be given by v_j and therefore its mobility must be given by qK_{ij}^{-1}. Generally, under a fixed orientation, the drift velocity will not be in the direction of the field. Overall, however, if all directions are equally probable, the distance traveled in the direction of the field would be given by the projection of v_j on the direction of $\underline{Ei}$ (average drift $<v_i>$) times the total displacement in time. This is shown in Figure 2 for two particles that are rotating at different speeds. As long as hypothesis (iv) is in effect, the average displacement regardless of the speed of rotation is taken from averaging Equation (6) as

$$x_i = \tau\ v_i = \frac{\tau q}{\overline{D_{ij}}}\ E_i = \tau q \overline{M_{ij}}\ E_i, \quad [14]$$

where τ is the total drift time.

Before describing the physical meaning of Equation (5), let us first interpret why Equation (4) and Equation (12) coincide. When Equation (6) is used, the right-hand side always yields the drag force ($F_D = K_{ij}v_j = D_{ij}v_i$) regardless of the value assigned to the angle θ. Every θ-rotation gives exactly the same information so the average of D_{ij} or K_{ij} must be equal even though K_{ij} is missing one orientation. This is similar to projecting v_j in the E_i direction.

However, when K_{ij} is inverted using Equation (3):

$$qK_{ij}^{-1}E_i = v_j, \quad [15]$$

rotating K_{ij}^{-1} an angle θ using E_i as the axis will yield different values of v_j given by $R_{Ei}v_j$ ($v_j \neq R_{Ei}v_j$). In such case, $\overline{(R_{E_i}K_{ij}^{-1}R_{E_i}^T)} \neq \overline{K_{ij}^{-1}}$ so that Equation (5) wrongly describes the average value of mobility in the direction of the field and should not be used.

An interpretation can nonetheless be extracted from Equation (5) by trying to calculate the displacement in the direction of the velocity. In such a case, the third orientation angle can be thought of a rotation using the velocity as an axis (instead of using E_i as in Equation (6)):

$$q\left(R_{v_j}K_{ij}^{-1}R_{v_j}^T\right)\left(R_{v_j}E_i\right) = v_j, \quad [16]$$

where R_{vj} in this case is the rotation of the ion and angle θ using as an axis the velocity v_j. Note that Equation (16) and Equation (6′) have very different meanings and yield different results when averaged. Averaging $\left(R_{v_j}K_{ij}^{-1}R_{v_j}^T\right)$ or K_{ij}^{-1} will yield in this case the same result and which coincides with Equation (5). Indeed, this is equivalent to H&B's approach that ultimately calculates the average "settling velocity" and should not be mistaken with calculating the average mobility in the direction of the field. Given that the ion's true displacement is in the direction of the velocity, one can define a true mobility displacement, x_j, different from the average displacement in the direction of the field x_i given by

$$x_j = \Delta t v_j = q\Delta t K_{ij}^{-1}\ E_i. \quad [17]$$

Since any angle θ used to rotate E_i is valid in Equation (16), we can choose the angle that makes E_i be a vector fixed in the horizontal direction as is shown in Figure 2. Averaging over the rest of possible orientations yields

$$x_j = \tau v_j = q\tau Z_2\ E_i, \quad [18]$$

where the $<x_j>$ is now termed true mobility displacement. $<x_j>$ is always larger or equal to $<x_i>$ and represents how much distance the ion has traveled regardless of direction *vs.* the average mobility displacement $<x_i>$, which represents the distance covered in the direction of the field. Perhaps, the intention of H&B was to define this true drift velocity (displacement), which they refer to as "settling velocity" and it was misinterpreted later to be the averaged displacement in the direction of the field. It is quite clear however that Z_2 cannot be used to calculate the electrical mobility of the particle given by a regular IMS instrument as regular instruments cannot interpret how far the ion deviates from the straight path given by a constant electric

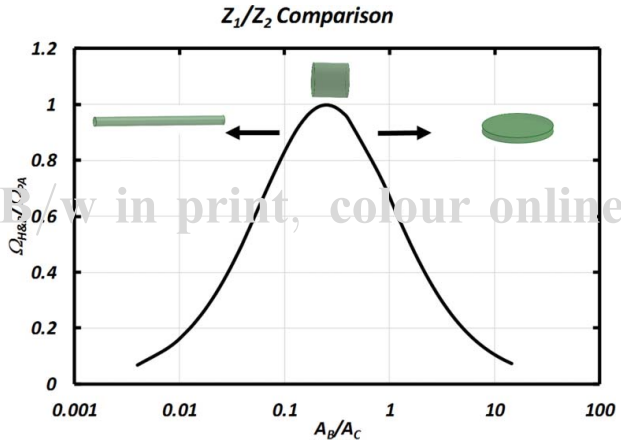

Figure 3. Ratio of $\frac{\Omega_{H\&B}}{\Omega_{PA}}$ (Z_1/Z_2) as a function of the ratio of A_B/A_C for a disk/cylinder molecule. Note that at $\frac{A_B}{A_c} = 1/4$, has its maximum value of 1.

field. Not even in such cases where an ion does not rotate at all during flight since the average displacement in the direction of the field would still be given by Equation (14).

3. Results and discussion

In order to understand the error associated with using Z_2 instead of using the corrected average Mobility Z_1, an analytical as well as a numerical method is employed. The analytical method calculates the true as well as the average mobility for a disk/cylinder and compares both. The numerical method *IMoS* has been used to demonstrate the validity of the theory for any structure (not only a disk/cylinder) using all atom models (see the SI). In particular, linear structures up to 1000 atoms and planar structures were studied up to 5000 atoms were computed using the Projected Area and Exact Hard Sphere Methods (EHSS). For the EHSS method, three different models of orientation for the ion are used to obtain independent values Z_1 and Z_2, which are then compared using Figure S1 and Table SI.

3.1. True vs. average electrical mobility of a disk/cylinder

The net drag force $d\vec{F}$ on an element of area dA with an outward normal is given by (de la Mora 2002):

$$\frac{d\vec{F}}{dA} = NkT\sqrt{\frac{8m_g}{\pi kT}}\vec{v}\cdot\left\{\overline{\overline{\mathrm{nn}}}\left(1-\frac{3a}{4}+\frac{a\pi}{8}\right)+\bar{\bar{I}}\frac{a}{4}\right\}. \quad [19]$$

Here N is number concentration, T is the temperature, k is the Boltzmann's constant, m_g is the mass of the gas (much smaller than the mass of the ion), $\overline{\overline{\mathrm{nn}}}$ is the normal diadic, $\bar{\bar{I}}$ is the unit diadic, and a is the accommodation coefficient.

For elastic and specular collisions ($a = 0$), the drag force can be written as

$$\vec{F} = \overline{\overline{K}}\cdot\vec{v}, \quad [20]$$

where the friction tensor $\overline{\overline{K}}$ is given by

$$\overline{\overline{K}} = NkT\sqrt{\frac{8m_g}{\pi kT}}\oint\overline{\overline{\mathrm{nn}}}dA \quad [21]$$

and where dA is integrated over the complete surface A_w of the ion.

In the case of a cylinder or a disk, with each of the bases having a surface A_B and side surface A_C, the friction tensor is given by

$$\overline{\overline{K}} = N\sqrt{\frac{8m_gkT}{\pi}}\oint\begin{bmatrix}\cos^2\theta & & \\ & \sin^2\theta & \\ & & 1\end{bmatrix}$$

$$dA = N\sqrt{\frac{8m_gkT}{\pi}}\begin{bmatrix}\frac{1}{2}A_c & & \\ & \frac{1}{2}A_c & \\ & & 2A_B\end{bmatrix}. \quad [22]$$

The average mobility depending on whether we use the average of the tensor or its inverse yields:

$$Z_1 = \frac{3ze}{4N}\sqrt{\frac{2\pi}{m_gkT}}\frac{1}{(A_c+2A_B)} \quad [23]$$

$$Z_2 = \frac{ze}{N}\sqrt{\frac{2\pi}{m_gkT}}\frac{8A_B+A_c}{24A_BA_c}. \quad [24]$$

We wish to compare the average of the friction tensor and/or its inverse with the well-known Mason–Schamp equation (repeated from Equation (1)):

$$Z_{M\&M} = \frac{3ze}{16N\Omega}\left(\frac{2\pi}{m_gkT}\right)^{1/2}. \quad [25]$$

Here, Ω, is the first collision integral, which, when specular and elastic collisions are considered and the body is convex (such as in the case of a cylinder or a disk), coincides with the average projected area of the ion. For a disk/cylinder, Cauchy's theorem states that

$$\Omega_{PA} = \frac{A_w}{4} = \frac{A_c+2A_B}{4}. \quad [26]$$

Using the above expression in the Mason–Schamp equation, one arrives at

$$Z_{M\&M} = \frac{3ze}{4N}\sqrt{\frac{2\pi}{m_g kT}}\frac{1}{(A_c + 2A_B)}, \quad [27]$$

which is exactly equivalent to Z_1. However, when Z_2 is compared to $Z_{M\&M}$, we arrive at the following equality:

$$\frac{6A_C A_B}{8A_B + A_c} = \frac{A_c + 2A_B}{3}, \quad [28]$$

which has a solution $A_B = A_c/4$ (or the diameter is equal to the length of the cylinder/disk). By analogy, one can term the collision cross-section from Z_2 as $\Omega_{H\&B} = \frac{9A_c A_b}{16A_B + 2A_c}$. Figure 3 shows the ratio $\frac{\Omega_{H\&B}}{\Omega_{PA}}$ (Z_1/Z_2) as a function of the ratio of A_B/A_C. As can be observed, $\Omega_{H\&B}$ is always equal or smaller than Ω_{PA} and they are only equal at the particular value specified. Moreover, the bigger the difference between A_C and A_B, the smaller the ratio becomes. A rotation of the tensor in Equation (22) using Equations (6–13) would lead to the tensor $K_{ii} = \frac{A_C + 2A_B}{3}$ and to the agreement of both mobilities in Equations (23) and (24).

4. Conclusions

In this manuscript, it is shown that previous approaches to calculate average collision cross-sections agree when the same considerations are applied. The previously used H&B approach using the inversion of the drag tensor assuming all directions are equally probable is shown to be invalid due to the omission of one of the angles of rotation of the ion in Equation (3). A small geometrical consideration to rotate the tensor in the axial direction of the electric force is sufficient to demonstrate that same identical results can be obtained through the tensor or the inverse. We show however that the H&B method gives instead a total displacement of the ion in the direction of the velocity, which we have termed the true mobility displacement to differentiate it from the average mobility displacement.

Analytical calculations of a disk/cylinder molecule show that the ratio between true and average mobility can be quite large. Indeed, there is only one value where the true mobility is equal to the average mobility of the ion. In all other cases, the mobility inferred using H&B, can be several times smaller than that inferred from using the average projected area.

Numerical calculations of the collision cross-section of linear and planar structures using four different approaches has been pursued using *IMoS*, a momentum transfer kinetic theory approach using all atom models. By calculating both H&B and M&M approaches and comparing them to the regular projected area approximations the inadequacy of the H&B method to predict average mobility values is confirmed.

Acknowledgments

Carlos Larriba Andaluz would like to acknowledge Juan Fernandez de la Mora for the fruitful discussions that have helped put together this manuscript.

ORCID

Carlos Larriba-Andaluz http://orcid.org/0000-0003-0864-7733

References

Alexander, A. L., Lee, J. E., Lazar, M., and Field, A. S. (2007). Diffusion Tensor Imaging of the Brain. *Neurotherapeutics*, 4(3):316–329.

Basser, P. J., Mattiello, J., and LeBihan, D. (1994). MR Diffusion Tensor Spectroscopy and Imaging. *Biophys. J.*, 66 (1):259–267. doi: 10.1016/S0006-3495(94)80775-1

Basser, P. J., and Pierpaoli, C. (2011). Microstructural and Physiological Features of Tissues Elucidated by Quantitative-Diffusion-Tensor MRI. (1996). *J. Magn. Reson.*, 213 (2):560–570. doi: 10.1016/j.jmr.2011.09.022

Bird, G. A. (1994). *Molecular Gas Dynamics and the Direct Simulation of Gas Flows*. Clarendon Press; Oxford University Press, Oxford, New York.

Bohrer, B. C., Mererbloom, S. I., Koeniger, S. L., Hilderbrand, A. E., and Clemmer, D. E. (2008). Biomolecule Analysis by Ion Mobility Spectrometry. *Ann. Rev. Anal. Chem.*, 1:293–327.

Chan, P., and Dahneke, B. (1981). Free−Molecule Drag on Straight Chains of Uniform Spheres. *J. Appl. Phys.*, 52 (5):3106–3110. doi: doi:http://dx.doi.org/10.1063/1.329173

Dahneke, B. E. (1973a). Slip Correction Factors for Nonspherical Bodies—I Introduction and Continuum Flow. *J. Aerosol Sci.*, 4(2):139–145. doi: http://dx.doi.org/10.1016/0021-8502(73)90065-7

Dahneke, B. E. (1973b). Slip Correction Factors for Nonspherical Bodies—II Free Molecule Flow. *J. Aerosol Sci.*, 4(2):147–161. doi: http://dx.doi.org/10.1016/0021-8502(73)90066-9

de la Mora, J. F. (2002). Free-Molecule Mobility of Polyhedra and Other Convex Hard-Bodies. *J. Aerosol Sci.*, 33(3):477–489.

de la Mora, J. F., de Juan, L., Eichler, T., and Rosell, J. (1998). Differential Mobility Analysis of Molecular Ions and Nanometer Particles. *Trac-Trends Anal. Chem.*, 17(6):328–339.

Epstein, P. S. (1924). On the Resistance Experienced by Spheres in their Motion through Gases. *Phys. Rev.*, 23:710. doi: http://dx.doi.org/10.1103/PhysRev.23.710

Garciaybarra, P., and Rosner, D. E. (1989). Thermophoretic Properties of Nonspherical Particles and Large Molecules. *AICHE J.*, 35(1):139–147.

Garcia-Ybarra, P. L., Castillo, J. L., and Rosner, D. E. (2006). Drag on a Large Spherical Aggregate with Self-Similar Structure: An Asymptotic Analysis. *J. Aerosol Sci.*, 37 (3):413–428.

Happel, J., and Brenner, H. (1981). *Low Reynolds Number Hydrodynamics with Special Applications to Particulate Media*. Springer Netherlands, Dordrecht.

Hogan, C. J., and de la Mora, J. F. (2011). Ion Mobility Measurements of Nondenatured 12–150 kDa Proteins and Protein Multimers by Tandem Differential Mobility Analysis-Mass Spectrometry (DMA-MS). *J. Am. Soc. Mass Spectrom.*, 22(1):158–172.

Jiang, J. K., Zhao, J., Chen, M. D., Eisele, F. L., Scheckman, J., Williams, B. J., Kuang, C., and McMurry, P. H. (2011). First Measurements of Neutral Atmospheric Cluster and 1–2 nm Particle Number Size Distributions During Nucleation Events. *Aerosol Sci. Technol.*, 45(4):Ii–V.

Landau, L. D., and Lifshitz, E. M. (1987). *Fluid Mechanics*. 2nd ed. Pergamon Press, Oxford, England; New York, pp. 227–237.

Larriba-Andaluz, C., Fernandez-Garcia, J., Ewing, M. A., Hogan, C. J., and Clemmer, D. E. (2015). Gas Molecule Scattering and Ion Mobility Measurements for Organic Macro-Ions in He Versus N-2 Environments. *Phys. Chem. Chem. Phys.*, 17(22):15019–15029.

Larriba-Andaluz, C., and Hogan, C. (2013). Novel Interfaced Approach to Mobility Calculations with Diffuse Scattering and Maxwell Rotational Distributions for Diatomic Gases in the Free Molecular Regime. *Abstr. Papers Am. Chem. Soc.*, 246.

Larriba-Andaluz, C., and Hogan, C. J. (2014). Collision Cross Section Calculations for Polyatomic Ions Considering Rotating Diatomic/Linear Gas Molecules. *J. Chem. Phys.*, 141(19). doi: 10.1063/1.4901890

Larriba, C., and de la Mora, J. F. (2012). The Gas Phase Structure of Coulombically Stretched Polyethylene Glycol Ions. *J. Phys. Chem. B*, 116(1):593–598.

Larriba, C., de la Mora, J. F., and Clemmer, D. E. (2014). Electrospray Ionization Mechanisms for Large Polyethylene Glycol Chains Studied Through Tandem Ion Mobility Spectrometry. *J. Am. Soc. Mass Spectrom.*, 25(8):1332–1345.

Larriba, C., and Hogan, C. J. (2013a). Free Molecular Collision Cross Section Calculation Methods for Nanoparticles and Complex Ions with Energy Accommodation. *J. Comput. Phys.*, 251:344–363.

Larriba, C., and Hogan, C. J. (2013b). Ion Mobilities in Diatomic Gases: Measurement versus Prediction with Non-Specular Scattering Models. *J. Phys. Chem. A*, 117 (19):3887–3901.

Larriba, C., Hogan, C. J., Attoui, M., Borrajo, R., Garcia, J. F., and de la Mora, J. F. (2011). The Mobility-Volume Relationship below 3.0 nm Examined by Tandem Mobility-Mass Measurement. *Aerosol Sci. Technol.*, 45(4):453–467.

Li, M. D., Mulholland, G. W., and Zachariah, M. R. (2014a). Rotational Diffusion Coefficient (or Rotational Mobility) of a Nanorod in the Free-Molecular Regime. *Aerosol Sci. Technol.*, 48(2):139–141.

Li, M. D., Mulholland, G. W., and Zachariah, M. R. (2014b). Understanding the Mobility of Nonspherical Particles in the Free Molecular Regime. *Phys. Rev. E*, 89(2), 022112.

Li, Z. G., and Wang, H. (2003a). Drag Force, Diffusion Coefficient, and Electric Mobility of Small Particles. I. Theory Applicable to the Free-Molecule Regime. *Phys. Rev. E*, 68 (6), 061206.

Li, Z. G., and Wang, H. (2003b). Drag Force, Diffusion Coefficient, and Electric Mobility of Small Particles. II. Application. *Phys. Rev. E*, 68(6), 061207.

Mackowski, D. W. (1994). Calculation of Total Cross-Sections of Multiple-Sphere Clusters. *J. Opt. Soc. Am. A-Opt. Image Sci. Vision*, 11(11):2851–2861.

Mackowski, D. W. (2006). Monte Carlo Simulation of Hydrodynamic Drag and Thermophoresis of Fractal Aggregates of Spheres in the Free-Molecule Flow Regime. *J. Aerosol Sci.*, 37(3):242–259.

Mason, E. A., and McDaniel, E. W. (1988). *Transport Properties of Ions in Gases*. John Wiley & Sons, New York.

Mesleh, M. F., Hunter, J. M., Shvartsburg, A. A., Schatz, G. C., and Jarrold, M. F. (1997). Structural Information from Ion Mobility Measurements: Effects of the Long-Range Potential (Vol 100, pg 16082, 1996). *J. Phys. Chem. A*, 101 (5):968–968.

Oberreit, D., Rawat, V. K., Larriba-Andaluz, C., Ouyang, H., McMurry, P. H., and Hogan, C. J. (2015). Analysis of Heterogeneous Water Vapor Uptake by Metal Iodide Cluster Ions Via Differential Mobility Analysis-Mass Spectrometry. *J. Chem. Phys.*, 143(10), 104204.

Ouyang, H., Larriba-Andaluz, C., Oberreit, D. R., and Hogan, C. J. (2013). The Collision Cross Sections of Iodide Salt Cluster Ions in Air via Differential Mobility Analysis-Mass Spectrometry. *J. Am. Soc. Mass Spectrom.*, 24(12):1833–1847.

Pease, L. F., Tsai, D. H., Zangmeister, R. A., Zachariah, M. R., and Tarlov, M. J. (2009). Use of Electrospray-Differential Mobility Analysis to Characterize Biologically Conjugated Nanoparticles. *Abstr. Papers Am. Chem. Soc.*, 237.

Ruotolo, B. T., Benesch, J. L. P., Sandercock, A. M., Hyung, S. J., and Robinson, C. V. (2008). Ion mobility-Mass Spectrometry Analysis of Large Protein Complexes. *Nature Protocols*, 3(7):1139–1152.

Shvartsburg, A. A., Hudgins, R. R., Dugourd, P., and Jarrold, M. F. (1997). Structural Elucidation of Fullerene Dimers by High-Resolution Ion Mobility Measurements and Trajectory Calculation Simulations. *J. Phys. Chem. A*, 101 (9):1684–1688.

Shvartsburg, A. A., and Jarrold, M. F. (1996). An Exact Hard-Spheres Scattering Model for the Mobilities of Polyatomic Ions. *Chem. Phys. Lett.*, 261(1–2):86–91.

Tammet, H. (1995). Size and Mobility of Nanometer Particles, Clusters and Ions. *J. Aerosol Sci.*, 26(3):459–475.

Tsai, D. H., Pease, L. F., Zangmeister, R. A., Tarlov, M. J., and Zachariah, M. R. (2009). Aggregation Kinetics of Colloidal Particles Measured by Gas-Phase Differential Mobility Analysis. *Langmuir*, 25(1):140–146.

Zhang, C. L., Thajudeen, T., Larriba, C., Schwartzentruber, T. E., and Hogan, C. J. (2012). Determination of the Scalar Friction Factor for Nonspherical Particles and Aggregates Across the Entire Knudsen Number Range by Direct Simulation Monte Carlo (DSMC). *Aerosol Sci. Technol.*, 46 (10):1065–1078.